

Legend

Definition 1: Reynolds Number Re

Compares advection of momentum to frictional acceleration.

$$Re = \frac{UL}{\nu}$$

Definition 8: Buoyancy Vector $\mathbf{B} 1/s^2$

$$\mathbf{B} = -\frac{\nabla \rho \times \nabla p}{\rho^2}$$

Definition 2: Rossby Number Ro

Compares advection of momentum to Coriolis acceleration.

$$Ro = \frac{U}{fL}$$

Definition 9: Kinetic Energy per mass $E_k m^2/s^2$ **Definition 3: Rhines Number R_{fi}**

Ratio of Rhines scale to horizontal scale.

$$R_{fi} = \frac{U}{\beta L^2} = \frac{a}{L} Ro$$

Definition 10: Mechanical Energy per mass $E_k m^2/s^2$

Sum of kinetic and potential Energy.

Definition 11: Rossby Radius $L_R m$

The *geostrophic wavelength*. $L_R = c/f$

Definition 4: Burger Number Bu

Ratio of relative vorticity to *stretching* vorticity.

$$\sqrt{Bu} = \frac{NH}{fL} = \frac{L_R}{L}$$

Definition 12: Steering Level z_S

The critical depth where the real part of the Doppler shifted phase speed $c_S(z_S) = c(z) - u(z) = 0$ vanishes. I.e. the depth where the Doppler shift creates a standing wave, causing the disturbances to grow in place instead of spreading in space, analogous to a *supersonic bang*.

Definition 6: gravitational acceleration g m/s²

Value of surface normal component of all body forces.

Definition 7: vorticity ω 1/s

Definition 13: Rhines Scale L_{fi} [m]

Scale at which earth's sphericity becomes important.

$$L_{fi}^2 = \frac{U}{\beta} \quad (1)$$

Assuming Gaussian shape:

$$h = Ae^{-(x/\sigma)^2/2}$$

with $A = a' + a = Ae^{-1/2} + a$

$$\begin{aligned} \frac{\partial h(\sigma)}{\partial x} &= -\frac{A}{\sigma} e^{-1/2} \\ &= -\frac{a'}{\sigma} \end{aligned}$$

hence

$$\begin{aligned} L_{fi} &= \sqrt{\frac{g}{f} \frac{\partial h}{\partial x} \frac{1}{\beta}} \\ L_{fi} &= \sqrt{\frac{ga'}{f\sigma\beta}} \end{aligned} \quad (2)$$

TODO:en detail:

$$\begin{aligned} \frac{\partial h(\sigma)}{\partial x} &= -\frac{A}{\sigma} e^{-1/2} \\ &= -\frac{a}{\sigma} \frac{e^{-1/2}}{(1 - e^{-1/2})} \\ &= \frac{a}{\sigma (e^{1/2} - 1)} \end{aligned}$$

hence

$$\begin{aligned} L_{fi} &= \sqrt{\frac{g}{f} \frac{\partial h}{\partial x} \frac{1}{\beta}} \\ L_{fi} &= \sqrt{\frac{g}{e^{1/2} - 1} \frac{a}{f\sigma\beta}} \end{aligned} \quad (3)$$

Definition 14: Gravity Wave Phase Speed cm/s

$$c = \sqrt{g'H}$$

Definition 15: Reduced Gravity $g'(x, y, z)$ m/s²

$$\text{In the layered model } g' = g \frac{\delta\rho}{\rho_0} = N^2 h$$

Definition 16: Surface/interface Displacement $\eta(x, y)$ m**Definition 17: Brunt Väisälä frequency N 1/s**

$$N^2 = g / \rho_0 \frac{\partial \rho}{\partial z}$$

Definition 18: Mean Layer thickness H_m **Definition 19: Layer Thickness/physical height of an isopycnal surface $h(x, y, t)$ m/h(x, y, ρ , t) m**

$$h = H + \eta \text{ (in the layered model)}$$

Definition 20: Planetary Vorticity Ω 1/s

$$\Omega = 4\pi/\text{day}_{fix*}$$

Definition 21: Latitude ϕ rad

Definition 22: Earth's Radius a m**Definition 23: Surface-Normal Planetary Vorticity Component $f_{1/s}$**

$$f = \textcolor{blue}{f}_z = \Omega \sin \phi z$$

Definition 24: Change of Planetary Vorticity with Latitude β 1/ms

$$f_l = \frac{\partial f}{\partial y} = \Omega/a \cos \phi$$

Definition 25: Okubo-Weiss Parameter O_w 1/s²

$$O_w = \text{divergence}^2 + \text{stretching}^2 + \text{shear}^2 - \text{vorticity}^2.$$

A negative value indicates vorticity dominated motion, whereas a positive value indicates deformation.

Definition 26: Sea Surface Height SSH m**Definition 27: Isoperimetric Quotient IQ**

$$IQ = A/A_c = \frac{A}{\pi r_c^2} = \frac{4\pi A}{U^2} \leq 1.$$

The ratio of a ring's area to the area of a circle with equal circumference.

Definition 28: Gaussian radius r m

$$(H - a) = H \exp \left(-\frac{A}{2\pi r^2} \right).$$

Twice the Gaussian standard-deviation.

a : amplitude

H : Gaussian amplitude

A : determined area

Definition 29: dynamic eddy scale σ m

Distance from eddy's center to the line of maximum orbital speed *i.e.* the zero-vorticity contour.

Definition 30: Run **aviso-MI**

7-day time-step aviso with method **MI**.

Definition 31: Run **aviso-MII**

7-day time-step aviso with method **MII**.

Definition 32: Run **pop2avi-MII**

7-day time-step POP remapped to aviso-geometry with method **MII**.

Definition 33: Run **POP-7day-MII**

7-day time-step POP with method **MII**.

Definition 34: Run **POP-1day-MII-Southern-Ocean**

1-day time-step aviso with method **MII**.

Southern Ocean Only.

Minimum Age: 30 [d]

Contour step raised to 2 [cm]

1

Results

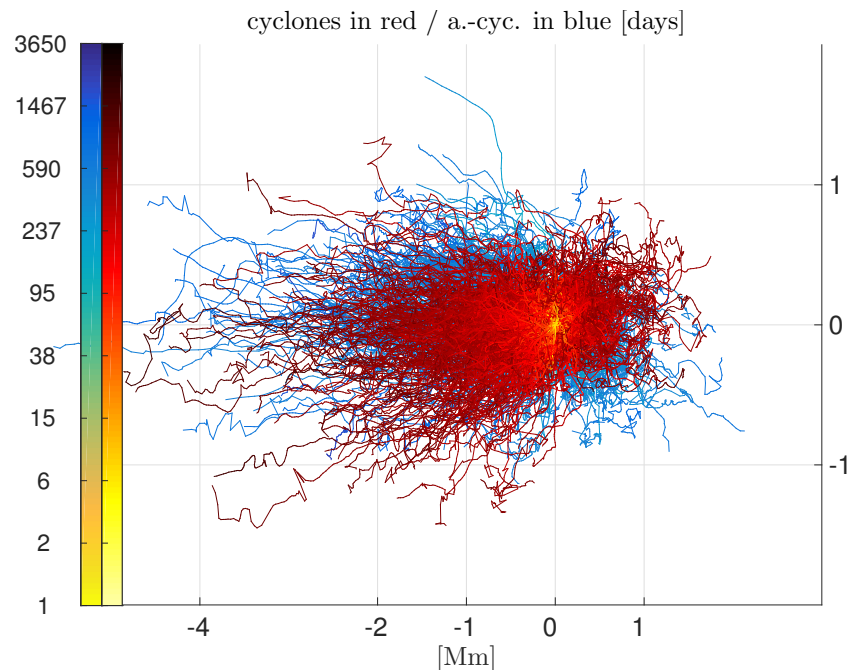


Figure 1.1: aviso-MI: Baseline-shifted old tracks. Tracks younger than 500days omitted.

The short time-frame and limited computational resources allowed for only a few complete global runs over the available data. It was therefore critical to carefully choose which method/parameters to use in order to maximize the deducible insight from the results. For best comparability of the results with each other it was decided to agree on one complete set of parameters as a basis, which would then be altered at key parameters. The first run is an attempt to reproduce

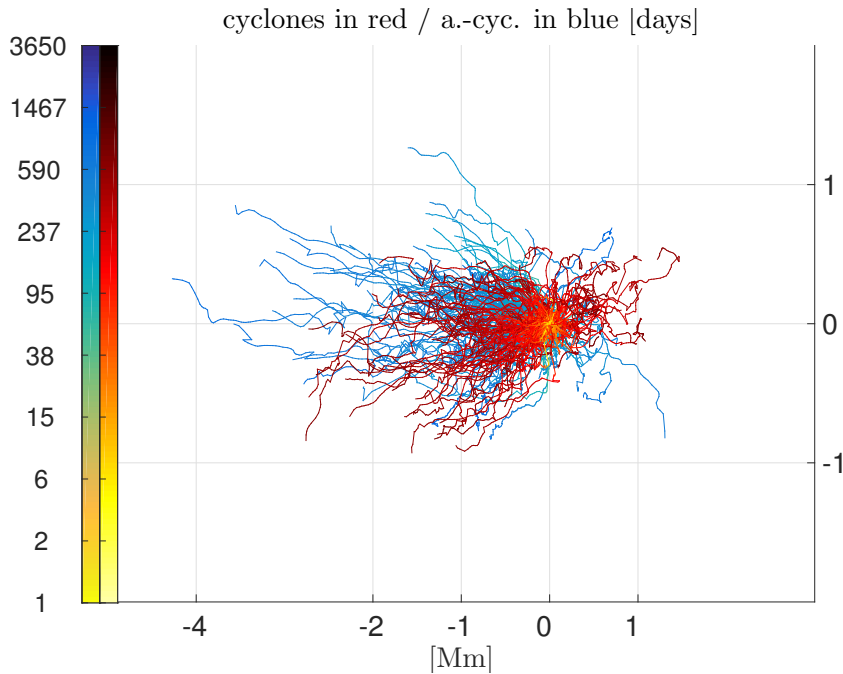


Figure 1.2: aviso-MII: Baseline-shifted old tracks. Tracks younger than 500days omitted.

the results from [?], by setting the algorithm to be the most similar to the algorithm described by [?]. The SSH-data for this run is therefore that of the Aviso product. This method will be called **MII**.

The second run is equivalent, except that this time the alternative **IQ**-based shape filtering method from TODO ref and the slightly different tracking-filter as described in TODO ref are used. This setting will be called **MII**. **MII** is then fed with 7-day time-step POP data as well.

To investigate what role space-resolution plays, the POP data was remapped to that of the Aviso data and fed to the **MII** method. Finally, to investigate the effects of resolution in time, an **MII**/3-day-time-step run over POP data was executed.

Start and end dates were fix for all runs as the intersection of availability of both data sets (see table ?? for details).

TODO lookup term used for krummes grid
TODO check tables for completeness

TODO:Chelton's identity check takes Leff?

time frame	1994/01/05 till 2006/12/27
scope	full globe (80S : 80N 180W : 180E)
AVISO geometry	641x1440 true Mercator
POP geometry	2400x3600
contour step	0.01
thresholds	[all SI]
max σ/L_R	4
min L_R TODO	20e3
min IQ	0.55
min data points of an eddy	8
max(abs(rossby phase speed)) TODO	0.2
max amplitude TODO	0.01

Table 1.1: Fix parameters for all runs.

Box 1. Method MI

The concepts used in this method are mostly based on the description of the algorithm described by [?] and all parameters are set accordingly. Basically MI is a modification of MII (which was completed first), with the aim to try to recreate the results from [?]. It differs from MII in the following:

- **detection**

As mentioned in TODO ref, the approach by [?] is to avoid overly elongated objects by demanding:

- high latitudes

The maximum distance between any vertices of the contour must not be larger than 400km for $|\phi| > 25^\circ$.

- low latitudes

The 400km -threshold increases linearly towards the equator to 1200km .

- **tracking**

The other minor difference to MII is in the way the tracking algorithm flags eddy-pairs between time-steps as sufficiently similar to be considered successful tracking-candidates (see TODO ref). In this method an eddy B from time-step $k+1$ is considered as a potential manifestations of an eddy A from time-step k as long as both - the ratio of amplitudes (with regard to the mean of SSH within the found contour) and the ratio of areas (interpolated versions as discussed in TODO ref) fall within a lower and an upper bound.

Box 2. Method MII

Even though, in its core, directly inspired by [?], this method differs from MII and thus from the description by [?] mainly in the way the shape of a found contour is deemed sufficiently eddy-like.

- **detection**

The IQ-method. See ?? and ??.

- **tracking**

Conceptually similar to MI, it is again vertical and horizontal scales that are compared between time-steps. Preferring a single threshold-value over one upper and one lower bound, a parameter ζ was introduced that is the maximum of the two values resulting from the two ratios of amplitudes respective σ , where either ratio is -if larger- its reciprocal in order to equally weight a decrease or an increase in respective parameter. In other words: $\zeta = \max([\exp|\log R_\kappa|; \exp|\log R_\sigma|])$, where R are the ratios.

1.1 MI - 7 day time-step - AVISO

THE RESULTS from the MI-method are special in that they feature many long-lived eddies (see ??????), some of which travelled more than 4000 km west. Tracks were recorded throughout the entire world ocean with the only exceptions being an approximately 20° -wide stripe along the equator. The highest count of unique eddies is along the Antarctic Circumpolar Current ¹ with counts of more than 60 individual eddy-visits per $1^\circ \times 1^\circ$ -cell. Further eddy-rich regions

¹ abbreviated ACC from here on.

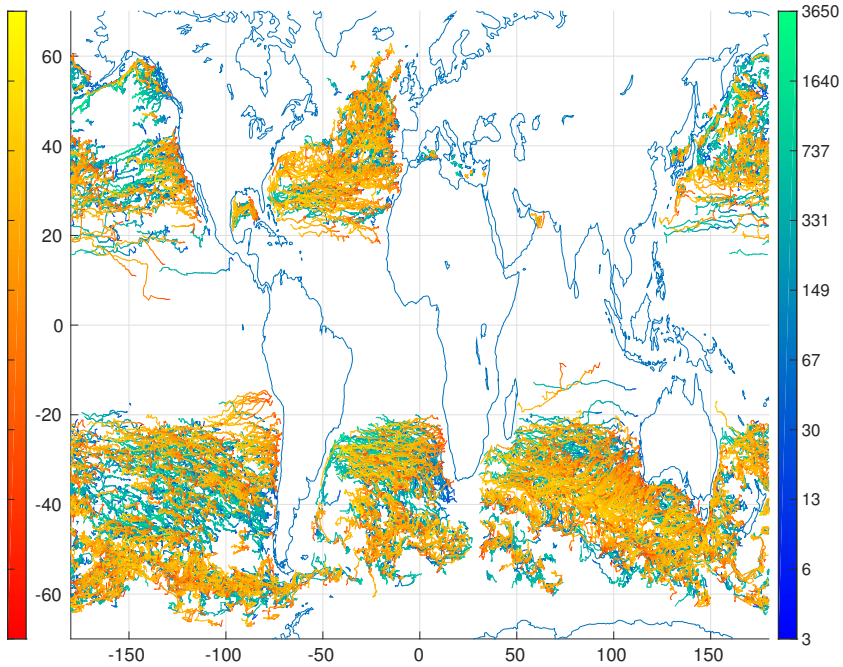


Figure 1.3: MI: anti-cyclones ind red. Tracks younger than 1a omitted for clarity.

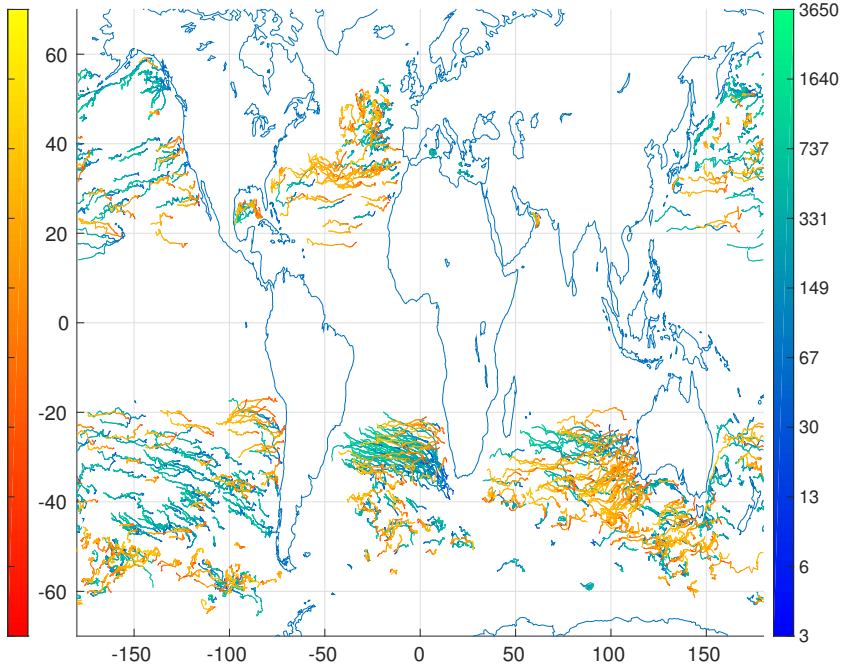


Figure 1.4: MII: anti-cyclones ind red. Tracks younger than 1a omitted for clarity.

are the western North-Atlantic throughout the Gulf-Stream and North-Atlantic Current, *Mozambique eddies* [?] at 20° South along the Mozambique coast, along the Agulhas Current and south of the Cup of Good Hope at $\sim 40^{\circ}$, along the coasts of Brazil, Chile and all along the Eastern, Southern and Western coasts of Australia (see ??).

EDDIES APPEAR AND DISAPPEAR throughout the world ocean. For long-lived solid eddies there is a tendency to emerge along western coasts (see ??).

THE SCALE σ of tracked eddies is similar to that in ?], yet generally smaller in high latitudes and slightly larger in low latitudes (see ??). It is larger than the first-mode baroclinic Rossby Radius by factor of at least 2 and its meridional profile appears to be separable into two different regimes; one apparently linear profile in low latitudes and a steeper one equatorwards of $\sim |15^{\circ}|$. Regionally, locations of high meso-scale activity appear to correlate with smaller eddy-scales (see ??).

THE EASTWARD ZONAL DRIFT SPEEDS are slightly slower than the first-mode baroclinic Rossby-Wave phase-speed and agree well with the results from ?]. Propagation is generally west-wards except for regions of sufficiently strong eastward advection as in the ACC and North Atlantic Current (see ???).

places of birth and death. size indicates final age.

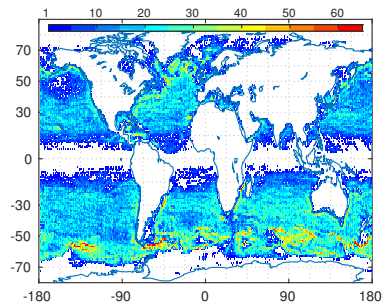
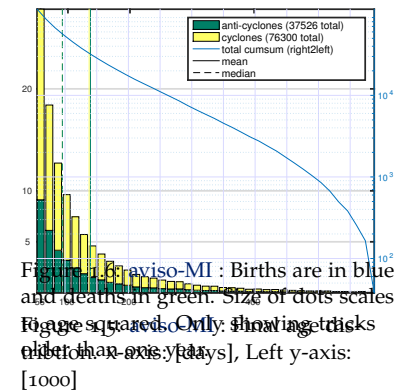
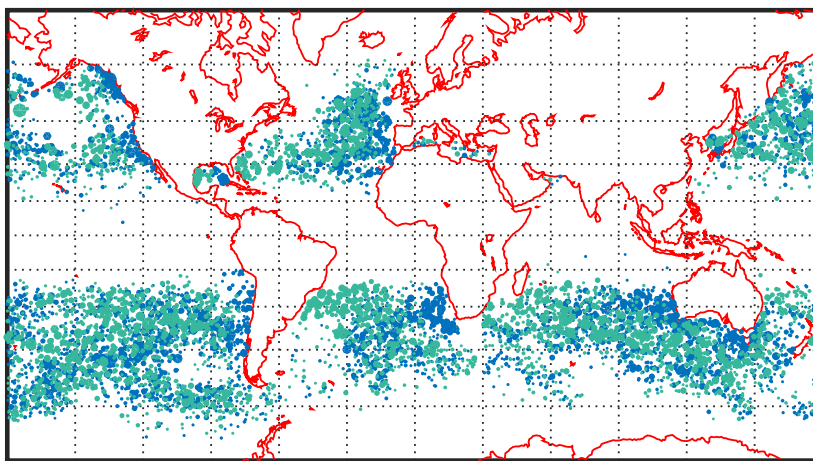
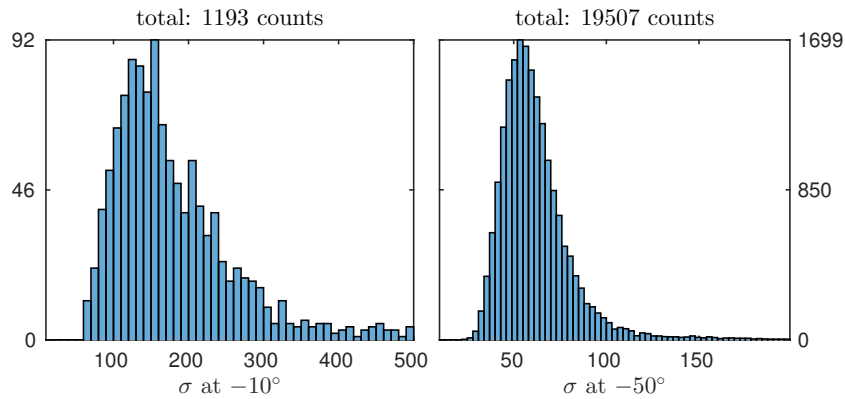
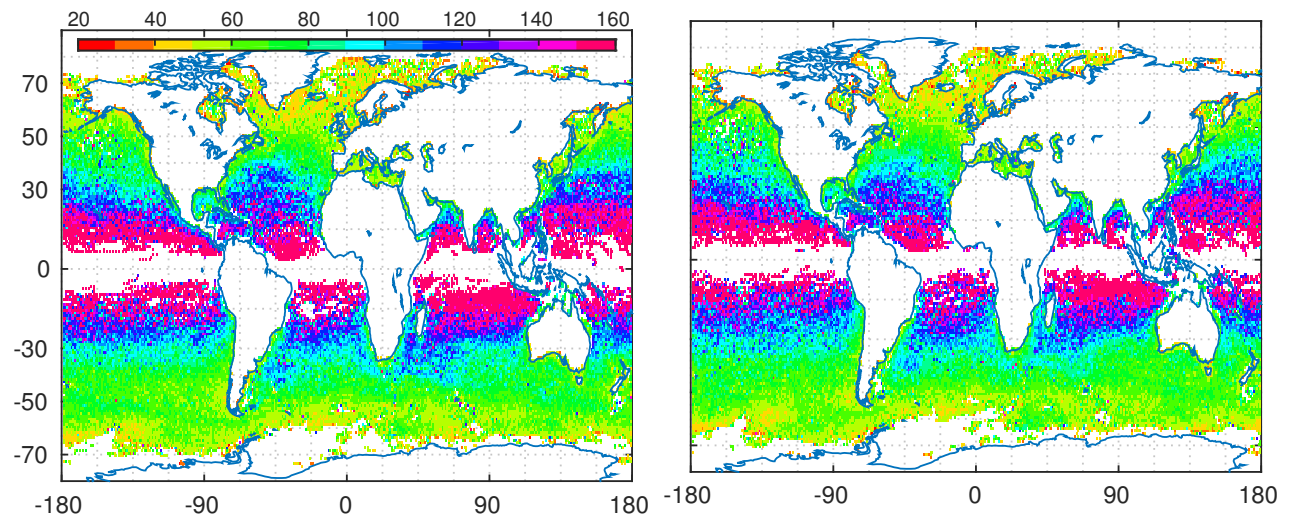


Figure 1.7: aviso-MI : Total count of individual eddies per 1 degree square.

Figure 1.8: [aviso-MI](#) : TODOFigure 1.9: [aviso-MI](#) : TODO

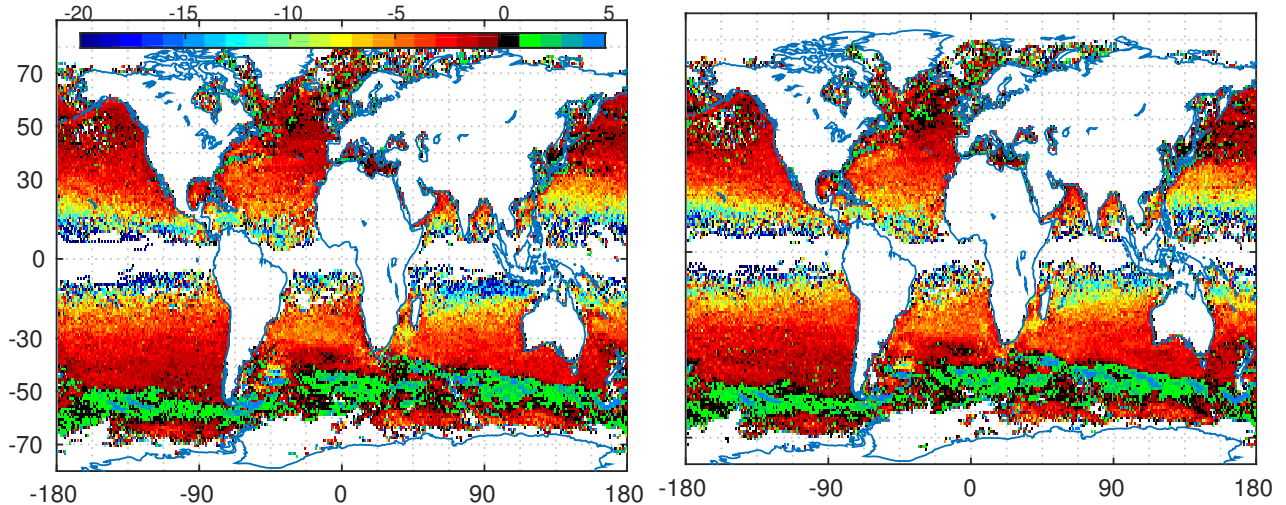


Figure 1.10: aviso-MI : TODO

1.2 MII - 7 day time-step - AVISO

THE IQ -BASED METHOD results in approximately the same total amount of tracks as the MI-method used in ?? (see ???). The difference is that tracks here are generally much shorter, meaning that less eddies are detected at any given point in time.

THE SCALE σ is now smaller than that from ?] for all latitudes in zonal- mean as well as median.

WESTWARD DRIFT SPEEDS are almost identical to those in ??.

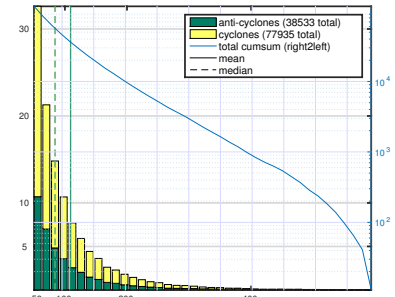


Figure 1.11: aviso-MII: Final age distribution. x-axis: [days], Left y-axis: [1000]

places of birth and death. size indicates final age.

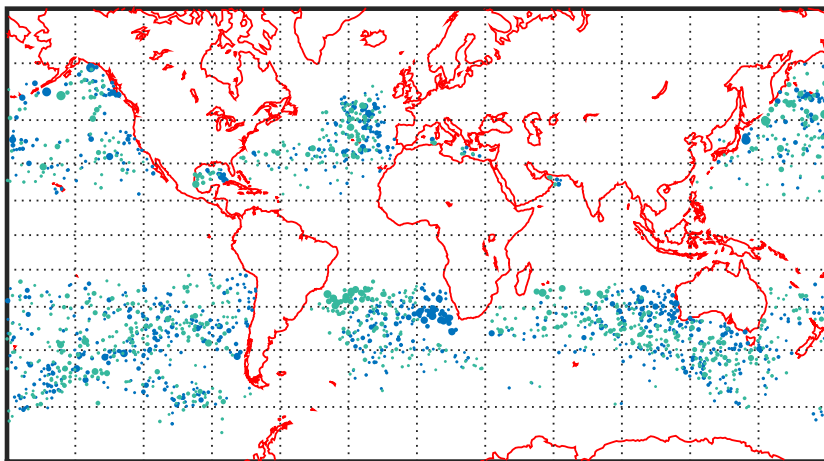


Figure 1.12: aviso-MII: Births are in blue and deaths in green. Size of dots scales to age squared. Only showing tracks older than one year.

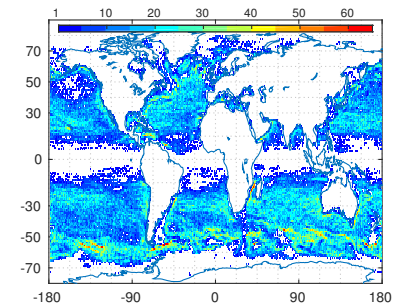


Figure 1.13: aviso-MII: Total count of individual eddies per 1 degree square.

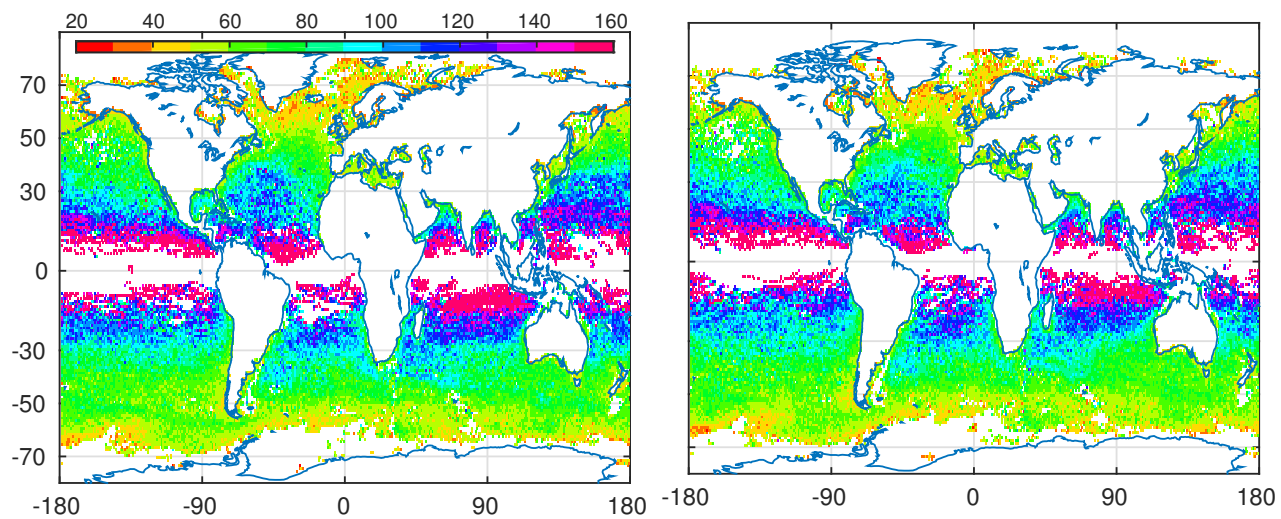


Figure 1.14: aviso-MII: TODO

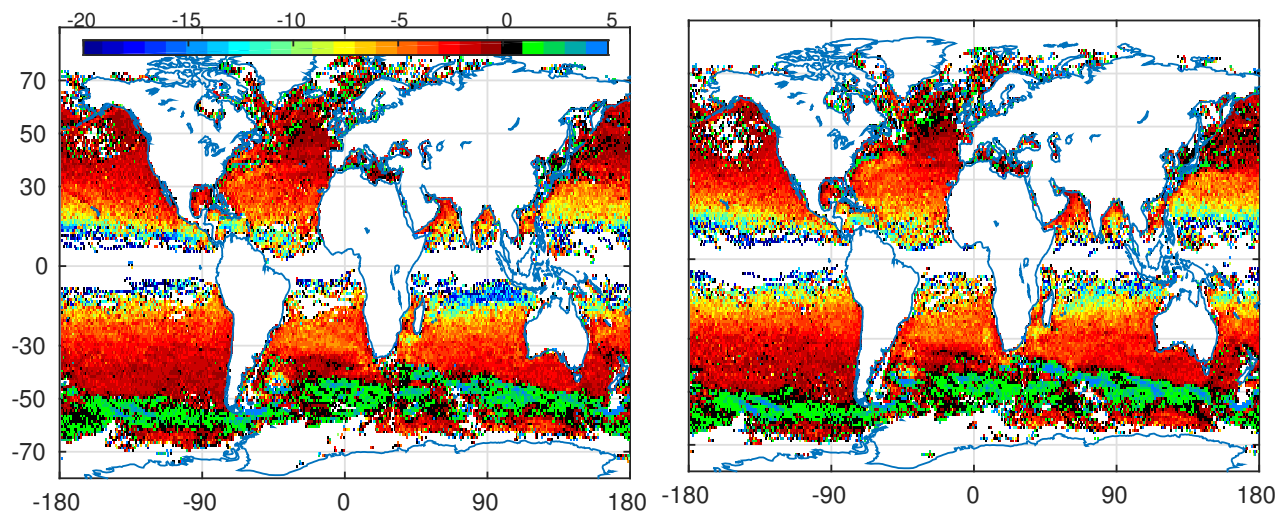


Figure 1.15: aviso-MII: TODO

1.3 MII - 7 day time-step - POP

THE MODEL DATA delivers slightly more total tracks with a similar 2-fold dominance of cyclones over anti-cyclones (compare ???). Similar to [aviso-MII](#) very long tracks are fewer than via [aviso-MI](#)². The regional pattern looks somewhat similar to the satellite patterns in terms of which regions feature the strongest eddy activity, with the exception of an unrealistic abundance of eddies right along the Antarctic coast where no eddies were detected for the satellite data likely due to sea ice and/or the inherent lack of polar data due to the satellites' orbit-inclinations. The more important difference between model- and satellite regional distributions is that the model results indicate significantly less eddy activity away from regions of strong SSH gradients, in the open ocean away from coasts and strong currents. The algorithm also detects hardly any eddy tracks in tropical regions (see ??).

THE SCALE σ is generally smaller for the model-data based analysis than for any satellite-based analyses, especially so in high latitudes.

WESTWARD DRIFT SPEEDS look regionally similar to those from satellite data (????). In the zonal mean their magnitude is below those from satellite (see ??).

² [aviso-MI](#) features 3000 tracks that are older than 400 days, while both [MII](#) methods have only ~ 1000 of such.

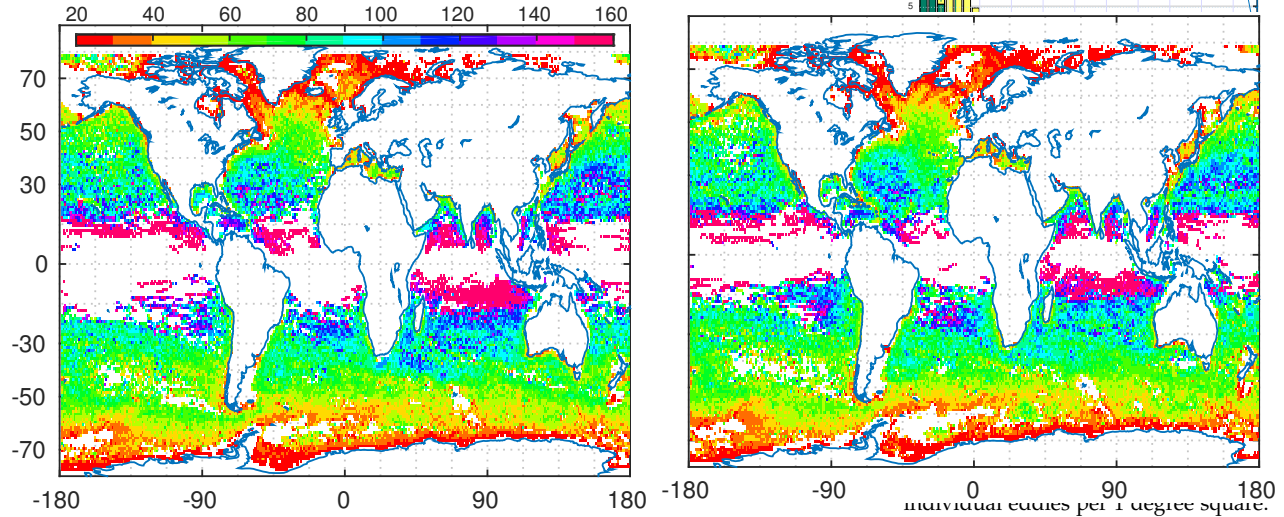


Figure 1.18: pop7-MII: TODO

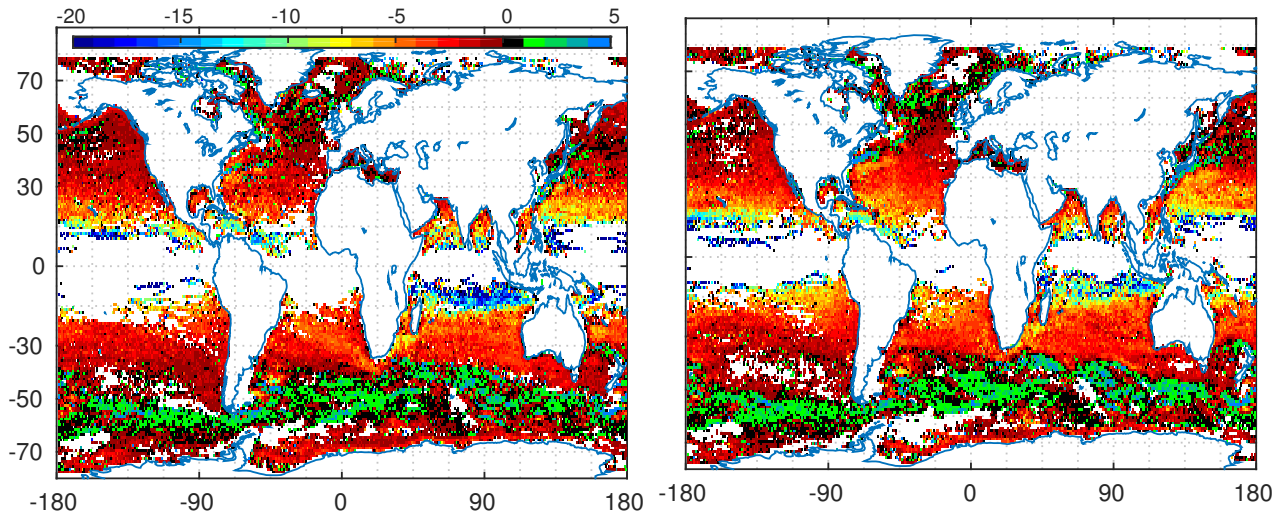


Figure 1.19: pop7-MII: TODO

1.4 MII - 7 day time-step - POP remapped to AVISO geometry

THE MODEL DATA

THE SCALE σ

WESTWARD DRIFT SPEEDS

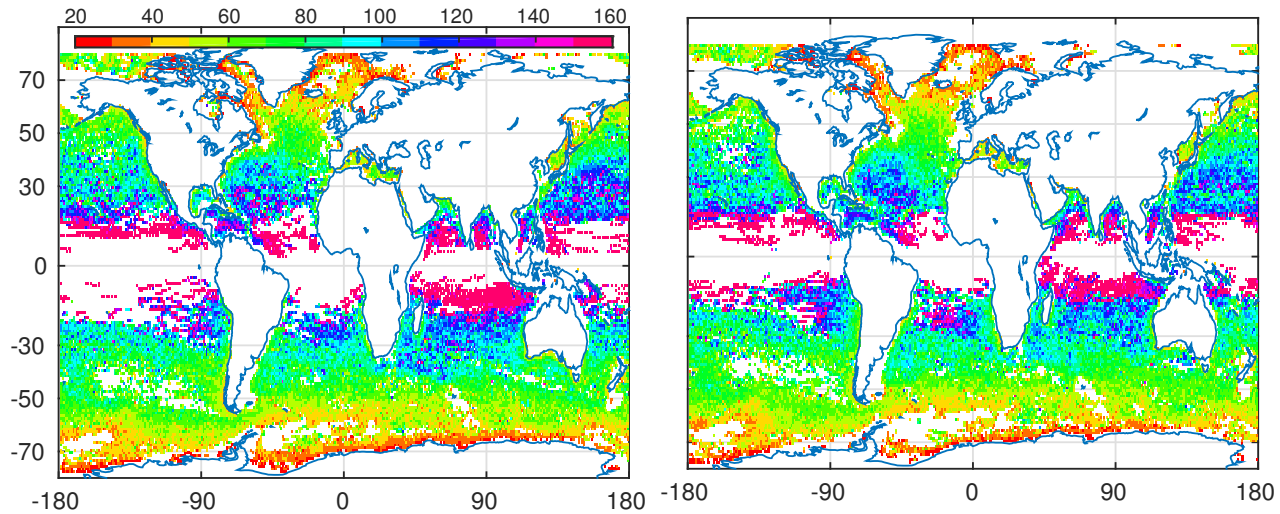


Figure 1.20: pop2aviso-MII: TODO

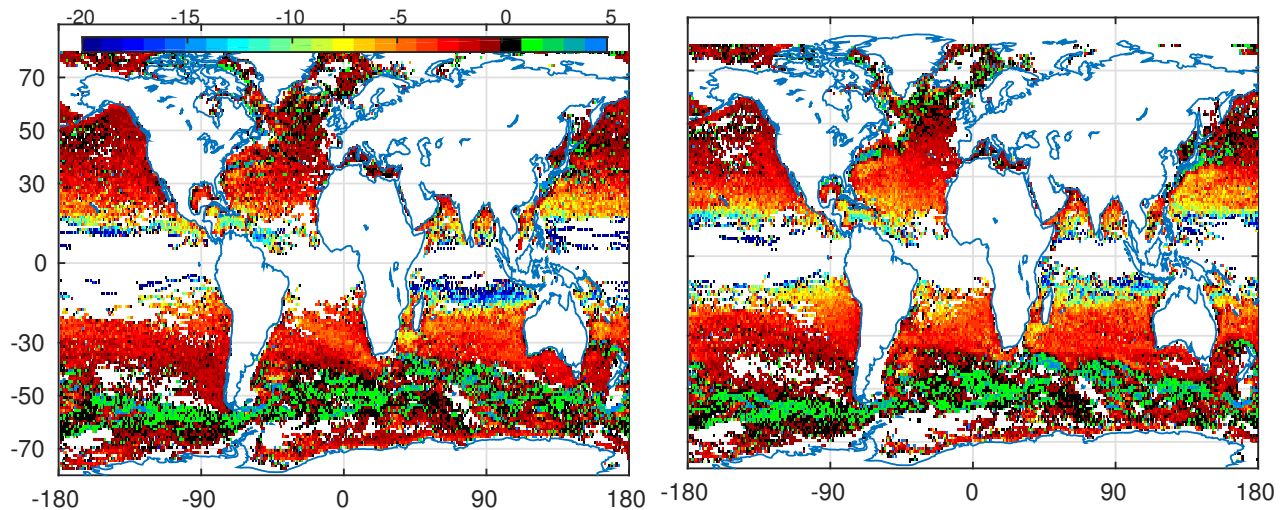


Figure 1.21: pop2aviso-MII: TODO

1.5 *MII - 1 day time-step - POP*

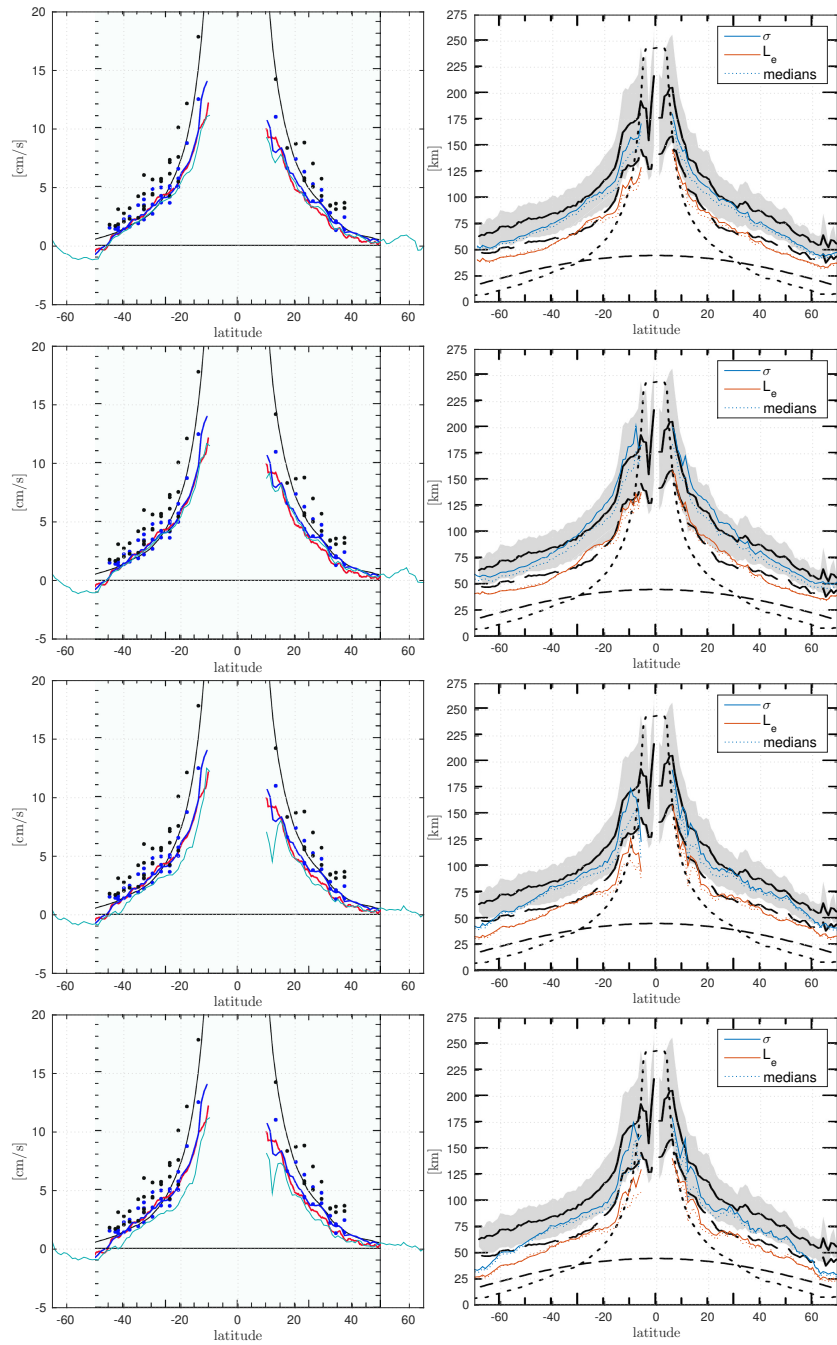


Figure 1.22: Left: Zonal-mean drift speed (cyan) fit to Fig 22 of [?] (Background). Right: σ and L_e fit to Fig. 12 of their paper. Dotted lines are medians instead of means. 1st row: **aviso-MII**, 2nd row: **aviso-MI**, 3rd row: **pop2avi-MII**, 4th row: **POP-7day-MII**

2

Discussion

2.0.1 Track Count and Lengths of Tracks

THE MOST APPARENT DIFFERENCE between the [two detection-methods](#) is the abundance of long-lived eddies resulting from the MI-method. The major difference between the two methods is the way in which the *shape* of found contour rings in SSH is decided to be sufficiently *eddy-like* or not [TODO:hlink](#).

THE MI-method is the more lenient one, as all it checks for, is whether the contour is of sufficiently compact form. The only shapes that are dismissed are long, thin elongated structures. This means that *e.g.* an eddy-track can more easily ¹ survive situations in which two eddies merge into one or those in which one is split into two or situations in which mean current gradients distort the vortex.

There could also be the situation in which an old, weak eddy fades, yet another one emerges in sufficient proximity. These two events would not even have to be at the exact same time, as long as some short-lived coherent structure, of which there is an abundance at any given time-step throughout the world ocean, acted as a *bridge* to fill the gap.

¹ as long as the similarity-criterion is not violated.

THE MII-method is conceptually different in that it is based on the assumption that a distinct coherent vortex need *per definition* to be more or less circular. It will therefor be more likely to regard *e.g.* the situation in which one eddy merges with another one as one of 3 eddies in total; **two** that have just died to create **one** new one. The focus here is more on the propagation of distinct circular

geostrophic vortices whereas the focus in the MI-method is more general on coherent local depressions respective elevations in SSH. Unfortunately the time-frame of this work did not allow to test to which degree tracers ² found within tracked eddies remained within the eddy over time. This could better clarify the assumption that the MI-method may be better at tracking water-mass advecting entities, with less jumps between bodies of water.

THE MI DETECTION METHOD a priori assumes that an eddy is more or less detected at its asymptotic *floor* *i.e.* in the case of an anti-cyclone at the *foot of the mountain*. The idea of the IQ -based method on the other hand is to assume that the situation of a single well-defined eddy sitting on an otherwise smooth, flat sea surface, which would be necessary for the contour algorithm to find a closed contour describing the outermost perimeter of said single vortex, is unrealistic. Instead the approach is to look for distinct, sufficiently circular *caps* of SSH- hills respepective valleys that consistently *wade* through all other weaker geostrophic noise surrounding it. **TODO: why gaussian or quad?**

TODO:diff maps etc

² in the model data.

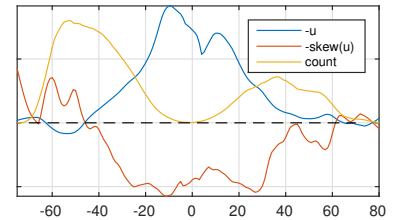


Figure 2.1: TODO

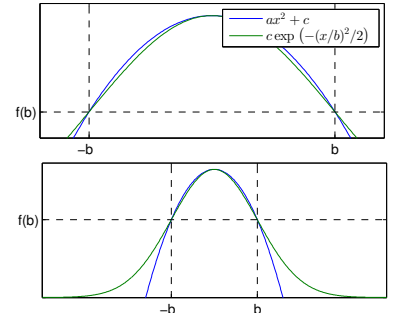


Figure 2.2: The upper part of a Gaussian profile can appear similar to a quadratic one.

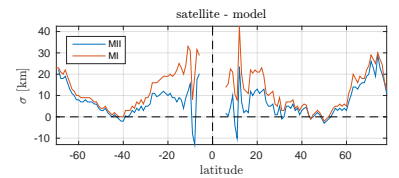


Figure 2.3: TODO:caption

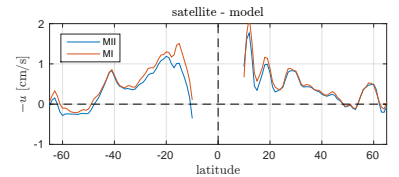


Figure 2.4: TODO:caption

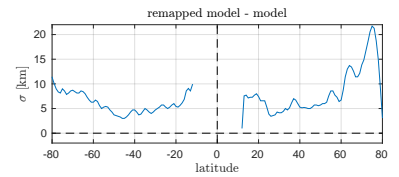


Figure 2.5: TODO:caption